

# Advances in Photoacoustic Imaging Reconstruction and Quantitative Analysis for Biomedical Applications

Lei Wang, Weiming Zeng\*, Kai Long, Rongfeng Lan, Li Liu, Wai Ting Siok, Nizhuan Wang\*

**Abstract**—Photoacoustic imaging (PAI) represents an innovative biomedical imaging modality that harnesses the advantages of optical resolution and acoustic penetration depth while ensuring enhanced safety. Despite its promising potential across a diverse array of preclinical and clinical applications, the clinical implementation of PAI faces significant challenges, including the trade-off between penetration depth and spatial resolution, as well as the demand for faster imaging speeds. This paper explores the fundamental principles underlying PAI, with a particular emphasis on three primary implementations: photoacoustic computed tomography (PACT), photoacoustic microscopy (PAM), and photoacoustic endoscopy (PAE). We undertake a critical assessment of their respective strengths and practical limitations. Furthermore, recent developments in utilizing conventional or deep learning (DL) methodologies for image reconstruction and artefact mitigation across PACT, PAM, and PAE are outlined, demonstrating considerable potential to enhance image quality and accelerate imaging processes. Furthermore, this paper examines the recent developments in quantitative analysis within PAI, including the quantification of haemoglobin concentration, oxygen saturation, and other physiological parameters within tissues. Finally, our discussion encompasses current trends and future directions in PAI research while emphasizing the transformative impact of deep learning on advancing PAI.

**Index Terms**—Photoacoustic imaging, Deep learning, Photoacoustic Image Reconstruction, Quantitative Analysis

## I. INTRODUCTION

### A. Fundamentals of Photoacoustic Imaging

Optical and ultrasound imaging are two well-established and advanced techniques that have become indispensable components of the medical imaging field [1]. Optical imaging, distinguished by its high sensitivity and robust contrast, has been extensively employed in biomedical research. However, the intrinsic limitations of optical diffusion presents a considerable challenge, hindering high-resolution imaging in

deep biological tissues and significantly limiting its potential for further advancement [2]. In contrast, ultrasound imaging (USI) has become a routine and essential method due to its low scattering properties within biological tissues [3], which offers several notable advantages, including high safety standards and strong penetration in medicine. These features are particularly beneficial for imaging the cardiovascular, abdominal, and digestive systems [4]. However, the minimal differences in acoustic-physical parameters among tissues result in low-contrast ultrasound images. Furthermore, the lack of microbubbles as contrast agents impedes the visualization of subtle changes in fine structures. It is therefore imperative to develop a novel imaging methodology that delivers high spatial resolution while effectively addressing the issue of imaging depth [5]. These technologies promise to combine the high contrast of optical imaging with the excellent penetrability of ultrasound imaging, thereby enabling more precise diagnosis and treatment monitoring in clinical settings [6], [7].

PAI employs the photoacoustic effect, seamlessly integrating optics and acoustics, and offers considerable potential for a wide range of applications [7], [8]. The physical basis of PAI is derived from the photoacoustic effect within biological tissues, whereby short-pulsed light is directly irradiated onto the tissue. The degree of light absorption depends on the wavelength of the light in question. Endogenous chromophores (e.g., DNA, RNA, haemoglobin, melanin, collagen, and lipids) or FDA-approved exogenous contrast agents (e.g., indocyanine green (ICG) and methylene blue) may be the source of the light. The absorption of each light pulse induces a rapid localized temperature increase, which results in thermal expansion and the generation of an ultrasound wave. The origin of this wave

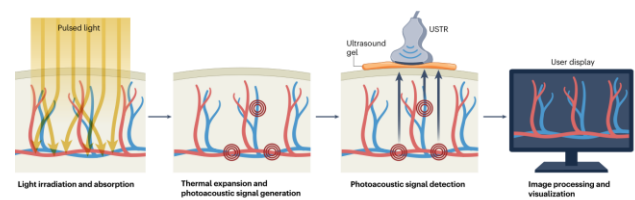


Fig. 1. The Complete Procedure of PAI [7].

This work was supported in part by the Hong Kong Polytechnic University Start-up Fund (Project ID: P0053210) and in part by Hong Kong RGC GRF under Grant 14220622 and Grant 14204321.

Lei Wang and Weiming Zeng are with the Laboratory of Digital Image and Intelligent Computation, Shanghai Maritime University, Shanghai, China. Lei Wang is also with the School of Electronic Engineering and Intelligent Manufacturing, Anqing Normal University, Anqing, China.

Kai Long and Li Liu are with School of Engineering, Great Bay University and Dongguan Great Bay Institute for Advanced Study, Dongguan, China.

Rongfeng Lan is with the Department of Cell Biology & Medical Genetics, School of Basic Medical Sciences, Shenzhen University Medical School, Shenzhen, China.

Wai Ting Siok and Nizhuan Wang is with the Department of Chinese and Bilingual Studies, The Hong Kong Polytechnic University, Hong Kong SAR, China. (\*correspondence e-mail: [wangnizhuan1120@gmail.com](mailto:wangnizhuan1120@gmail.com) or [zengwm86@163.com](mailto:zengwm86@163.com)).

can be identified by its time-of-flight. The ultrasound waves, which are known as photoacoustic waves, provide valuable information about the optical absorption properties of the tissue in question. An ultrasound transducer (USTR) detects the photoacoustic signals, which are then processed to generate cross-sectional 2D or 3D photoacoustic images. As illustrated in Fig. 1, the PAI procedure comprises the following steps: pulsed laser emission, light absorption, thermal expansion, ultrasonic wave generation, ultrasonic detection, and image reconstruction [7], [19].

Specifically, the stress relaxation time denotes the time required for the stress (pressure) to dissipate from the heated volume [7]. When the laser pulse duration is shorter than the stress relaxation time, stress confinement is indicated; when thermal confinement is also realized, the fractional volume expansion ( $\Delta V/V$ ) is negligible [10], as long as the following condition are satisfied:

$$\frac{\Delta V}{V} = -\kappa \Delta p + \beta \Delta T = 0, \quad (1)$$

where  $\Delta p$  and  $\Delta T$  represent the pressure and temperature change respectively;  $\kappa$  represents isothermal compressibility, and  $\beta$  denotes the thermal coefficient of volume expansion. Further, the initial local pressure rise ( $p_0$ ) after laser excitation can be calculated as:

$$p_0 = \frac{\beta}{\kappa \rho C_v} \eta_{th} \mu_a F = \Gamma \eta_{th} \mu_a F = \Gamma E_a, \quad (2)$$

where  $\rho$  denotes the mass density,  $C_v$  is the specific heat capacity at a constant volume,  $\eta_{th}$  is the percentage of specific optical absorption that is converted to heat,  $\mu_a$  is the optical absorption coefficient,  $F$  is the optical fluence, and  $E_a$  is the absorbed optical energy. Thus, the initial local pressure rise is directly proportional to the non-radiative optical energy absorption via the proportionality factor  $\Gamma$ , known as the Grüneisen coefficient.

### B. Advances of PAI

Biomedical imaging techniques, including computed tomography (CT), magnetic resonance imaging (MRI), positron emission tomography (PET), optical imaging (OI), and USI [6], are of paramount importance in the field of medicine. They provide comprehensive anatomical and physiological insights that are essential for disease diagnosis, treatment planning, and early detection of health risks [11]. However, these techniques are not without limitations, including diagnostic specificity, imaging velocity, patient exposure to ionizing radiation, and reliance on contrast agents.

PAI represents an emerging modality that overcomes the depth limitations of traditional OI, which is restricted by light diffraction to depths of less than 1 mm [12]. PAI unites the high sensitivity of optical imaging with the deep penetration of ultrasound, thereby conferring advantages such as high resolution, rapid imaging, and increased imaging depth [13]. This enables the visualization of deeper biological tissues while maintaining high contrast, thus rendering it a valuable tool for the study of the morphological, physiological, pathological and metabolic characteristics of tissues [14]. The selection of an appropriate contrast agent is of paramount importance for the enhancement of image specificity in PAI. While exogenous contrast agents are renowned for their high sensitivity and capacity to target specific molecules, endogenous agents such

as haemoglobin, lipids, melanin and water are preferred for non-invasive imaging due to their natural presence and non-toxic properties [15]. It is important to note that an increase in the central frequency and bandwidth of ultrasound enhances spatial resolution, but typically results in a reduction in imaging depth [16].

Despite the presence of challenges such as acoustic attenuation, coupling stability, bandwidth limitations, and electromagnetic interference, PAI is distinguished by its non-invasiveness, lack of ionising radiation, high contrast, and high spatial resolution, which collectively offer significant potential in biomedical research [17]. The sensitivity and resolution of PAI are contingent upon a number of factors, including the optical absorption contrast of the tissue, the duration of the laser pulse, and the precision of the image reconstruction algorithm [18]. It is therefore imperative that high-quality image reconstruction algorithms are developed in order to guarantee the quality of PAI imaging. Since its inaugural successful application in imaging the brains of live mice in the early 21st century, PAI has undergone considerable advancement in device development, algorithm optimization, and functional imaging [19]. Table 1 presents a comparative analysis of various imaging modalities [20].

As demonstrated in Table 1, PAI is capable of overcoming the inherent limitations of both optical coherence tomography (OCT) and USI, most notably the absence of speckle artefacts. By leveraging the photoacoustic effect, PAI is able to enhance tissue contrast and integrate ultrasonic detection, thereby facilitating high-resolution imaging. Furthermore, it reconstructs the distributions of optical absorption and attenuation coefficients, thereby enabling the quantification of blood oxygen saturation levels [21]. Furthermore, Fig. 2 demonstrates the resolution and depth characteristics of a range of imaging modalities, including ultrasound, optical, and photoacoustic imaging. In conclusion, PAI demonstrates considerable promise in biomedical research and clinical applications, providing high-contrast, high-resolution imaging with the capacity for deep-tissue measurement.

## II. KEY IMPLEMENTATIONS OF PAI

Advancements in laser technology between the late 1970s and early 1980s catalyzed pioneering studies on the

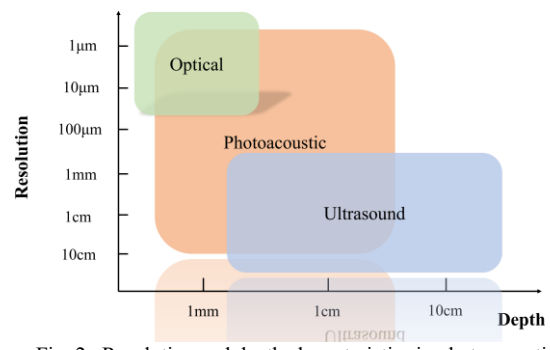


Fig. 2. Resolution and depth characteristics in photoacoustic, ultrasonic, and optical imaging.

photoacoustic effect, thereby establishing a robust foundation for the subsequent development of PAI [21]. By the early 21st century, several photoacoustic techniques, including PACT, PAM, and PAE, had reached a mature stage of development [22], [23]. These innovations represent a significant advancement in PAI and considerably expand the biomedical applications of the photoacoustic effect, thereby opening up new avenues for research and clinical practice [24]. Fig. 3 illustrates the three principal methodologies employed in PAI [25].

#### A. PACT

PACT is one of the earliest-developed imaging techniques, offering a radiation-free and safe approach for human imaging, [26], [27]. The technique has the potential to expand the fields of view that can be imaged and enhance the penetration capabilities of imaging, which could be beneficial for a number of biomedical applications. One such application is the quantitative analysis of blood oxygen saturation ( $sO_2$ ) in cancer diagnosis [14], [28].

PACT employs a wide-diameter, non-focused pulsed laser beam to illuminate tissue surfaces, with a non-focused array of ultrasonic detectors capturing the generated photoacoustic signals [22]. The signals are then processed via inversion algorithms to reconstruct the initial acoustic field, thereby producing high-resolution images across biological scales, from cellular to organ level, with detail resolution in the range of hundreds of micrometers [29], [30]. This technique offers a moderate spatial resolution, significant penetration depth, and rapid imaging speeds. The selection of an appropriate ultrasonic transducer array is dependent upon the specific application. Linear arrays are well suited to the scanning of small animals or surface tissues, whereas hemispherical arrays are more appropriate for broader human imaging, particularly in the context of breast cancer detection [31], [32]. The pivotal role of PACT in breast cancer detection has led to considerable advances in clinical research, with multiple systems currently in development for this purpose [33]. While PACT is an effective imaging technique with depth capabilities, its resolution is relatively moderate [34]. Additionally, contrast mechanisms differ between macroscopic and microscopic imaging [17]. Table 2 provides a comprehensive overview of the advantages and constraints of PACT.

In order to further enhance the potential of PACT, researchers have made significant advances in the development of imaging devices, contrast agents and models [35]. PACT

TABLE 2. ADVANTAGES AND CONSTRAINTS OF THE PACT MODALITY.

Modality	Advantages	Constraints
PACT	Radiation-free and safe; Wide field of view; Non-invasiveness; Greater imaging depth; Fast imaging speed; Moderate spatial resolution; Suitable for cellular to organ imaging.	Trade-off challenge between cost and SNR; Less prominent resolution; Differences in macro-micro contrast.

employs reconstruction algorithms to transform photoacoustic signals into acoustic source distributions, thereby generating images [36]. These algorithms are of pivotal importance in this field and exert a direct influence on imaging precision [37]. However, practical applications are confronted with challenges such as sparse angular views and limited bandwidth, which have the potential to impair image quality [36], [38]. In essence, the reconstruction process in PACT constitutes an acoustic inverse problem, which presents significant challenges due to incomplete data acquisition. It is therefore imperative to optimize existing technologies and develop new strategies if PACT is to advance in biomedical imaging [39].

#### B. PAM

Over the past decade, PAM has become a vital tool for microscopic imaging, utilizing its distinctive optical absorption contrast mechanism [27], [30]. As a versatile biomedical technique, PAM facilitates structural, functional, and molecular imaging using both endogenous and exogenous contrast agents. It has been widely applied in various fields, including blood flow perfusion, oxygenation imaging, tumor imaging, and brain imaging, utilizing haemoglobin as an endogenous absorber [38], [40]. In comparison to the centimeter-level penetration depth of PACT systems, PAM offers superior imaging resolution at similar depths [18], [33]. PAM employs focused short-pulse laser illumination and collects photoacoustic signals at discrete points using a focused ultrasound transducer. The data acquisition system amplifies and samples these signals, forming the image progressively during point-by-point scanning, thereby eliminating the need for additional inversion algorithms. This makes the system invaluable for biomedical applications. By circumventing light scattering, PAM is capable of surpassing the high-resolution optical imaging depth limit of approximately 1 millimeter, thereby achieving high-resolution imaging of deep tissues [31]. PAM is particularly suited to high-precision imaging of skin and tissue surfaces, with a resolution of up to the micron level [31].

The categorization of PAM is based on the relative sizes of the optical and acoustic beam focuses, resulting in two types: optical-resolution PAM (OR-PAM) and acoustic-resolution PAM (AR-PAM) [5], [18], [25]. OR-PAM utilizes a tightly focused light source, thereby achieving high lateral resolution (less than 5  $\mu\text{m}$ ), which is determined by the optical spot size. However, its penetration depth is limited to 1-2 millimeters due to light scattering. In contrast, AR-PAM utilizes weakly focused or collimated light beams, with lateral resolution defined by the acoustic focal spot. This enables deeper imaging (approximately 3-10 millimeters) but with reduced lateral resolution ( $>50 \mu\text{m}$ ) and increased background noise. The axial resolution of both OR-PAM and AR-PAM is contingent upon

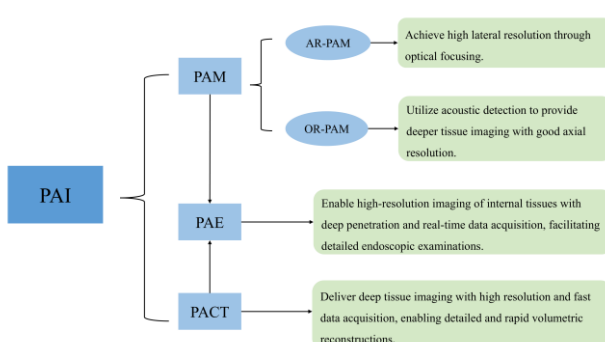


Fig. 3. Three Key Implementations of PAI.

the bandwidth of the ultrasound transducer. The principal challenge facing PAM is to attain high lateral resolution in AR-PAM without sacrificing imaging depth. Furthermore, the majority of OR-PAM systems employ mechanical scanning for both optical excitation and ultrasound detection, which restricts the imaging speed. Nevertheless, OR-PAM has demonstrated utility in biomedical research domains, including tumor angiography and melanoma cell imaging [31], [41]. For imaging depths exceeding one millimeter, AR-PAM is particularly effective in deep penetration imaging, overcoming the limitations of light diffusion. AR-PAM is a versatile technique that can be employed to obtain a range of biomedical data, including measurements of oxygenated and deoxygenated haemoglobin concentrations, blood flow velocity, and oxygen metabolism rates [20].

A principal technical challenge for PAM is the balancing of spatial resolution and imaging speed [41], [42]. The clinical adoption of PAM has been impeded by a number of factors, including the use of high laser excitation doses, the limitation of imaging speeds, and the suboptimal quality of the images produced [17], [31]. The parameters of laser dose, imaging speed and image quality are interdependent. The current approach is to develop advanced image and signal processing models with the objective of enhancing image quality [43]. Table 3 provides a comprehensive overview of the advantages and constraints of PAM.

### C. PAE

The applicability of traditional PACT and PAM is relatively limited for imaging internal tissues and organs, such as those within the digestive system and vascular walls. To address this limitation, researchers have integrated non-invasive photoacoustic tomography with endoscopic technology, thereby enabling the imaging of deep internal tissue structures

TABLE 4. ADVANTAGES AND CONSTRAINTS OF THE PAE MODALITY.

Modality	Advantages	Constraints
PAE	Non-invasive; Suitable for internal imaging; High-quality imaging of shallow tissue; Miniatized system for <i>in vivo</i> use; Aids in lesion detection and diagnosis.	Limited spatial resolution; Restricted field of view; Susceptibility to noise; Interference from background tissues; Signal attenuation.

[19], [44]. Although PAE is the most recent of these three PAI techniques, it has developed rapidly and is capable of imaging internal tissues, including the digestive tract, blood vessels, and the urogenital system. Consequently, PAE has emerged as a significant area of research [44].

PAE is particularly well-suited for the detection of lesions in biological cavities, including the nasal cavity, digestive tract, and arterial vessels. It provides high-quality images of superficial tissues, which are useful for the diagnosis of various conditions. PAE employs the use of miniaturized MEMS scanning devices and fiber optic sensors, which serve to reduce the overall system size, thereby facilitating the implementation of *in vivo* imaging procedures. This enables physicians to examine organ conditions or lesions for diagnostic purposes. However, due to spatial constraints within the lumen, the detector is only capable of collecting photoacoustic signals within a limited angular range, which may have an adverse effect on the quality of the reconstructed image. Table 4 provides a comprehensive overview of the advantages and constraints of PAE. In conclusion, a comparison of the characteristics of the three principal PAI modalities is provided in Table 5.

TABLE 5. CHARACTERISTIC COMPARISON OF THREE MODALITIES OF PAI.

Modalities	Resolution	Range	Depth	Cost
PACT	Low	Large	Deep	Expensive
AR-PAM OR-PAM	High	Limited by scanning range	Shallow	General
PAE	High	Shallow	Shallow	General

The following sections will focus on image reconstruction techniques, including both conventional and deep learning methods, for PAI, as well as a quantitative analysis of PAI, as illustrated in Fig. 4.

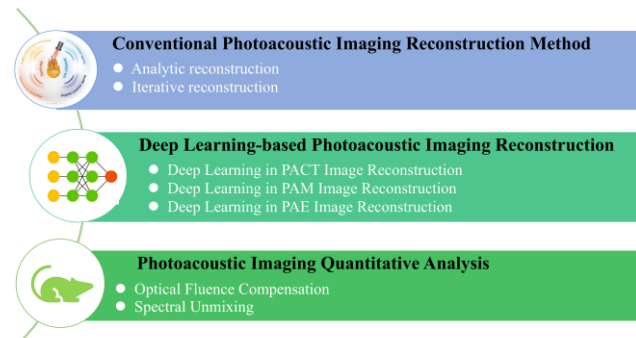


Fig. 4. Illustrative overview outlining the scope of this review.

Characteristics	OR-PAM	AR-PAM
<b>Advantages</b>		
Lateral Resolution	High (<5 $\mu\text{m}$ ) Determined by ultrasound transducer bandwidth	Moderate (>50 $\mu\text{m}$ ) Determined by ultrasound transducer bandwidth
Axial Resolution		
Depth Penetration	Limited (~1-2 mm)	Deeper (~3-10 mm)
Contrast Mechanism	Strong optical focusing enhances contrast	Applicable for broader imaging applications
Imaging Precision	Suitable for high-precision surface imaging	Suitable for deeper tissue imaging
<b>Constraints</b>		
Depth Penetration	Restricted by light scattering effects	Limited by reduced lateral resolution and increased background noise
Lateral Resolution	Not suitable for deep tissue imaging	Lower compared to OR-PAM
Imaging Speed	Mechanical scanning limits speed	Can be slower due to the broader imaging area
Contrast Noise Ratio	Can suffer from low contrast in deeper tissues	May have higher background noise affecting the clarity
Clinical Application	Limited by the depth and speed constraints	Challenges include lower resolution and noise in deeper tissues

### III. CONVENTIONAL RECONSTRUCTION IN PAI

The core principle of PAI is to map the distribution of optical absorption coefficient distribution within tissues, which is directly correlates with the initial acoustic pressure distribution. Developing robust reconstruction models is essential for accurately inverting the initial acoustic pressure from the acquired photoacoustic signals [45].

Conventional reconstruction methods can be broadly classified into analytical and iterative (shown in Fig. 5) [46]. In addition, analytical reconstruction utilizes time and frequency domain methods to identify optimal solutions, among which are models such as time reversal (TR) [47], [48], delay-and-sum (DAS) [49], [50] in the time domain, and filtered back projection (FBP) [51] in the frequency domain.

High-fidelity image reconstruction is pivotal to enhancing the accuracy of photoacoustic imaging, transforming the raw signals received by ultrasonic transducers into images of initial pressure distributions [52]. When data acquisition is incomplete, conventional PAI imaging reconstruction methods such as back-projection [53], TR, and DAS may result in diminished image quality and reduced imaging depth [54].

Conversely, iterative reconstruction utilizes optimization techniques or regularization to solve underlying linear equations, offering higher signal-to-noise ratios (SNR) and improved image quality despite their computational intensity. These methods assume ideal conditions such as high temporal and spatial sampling, complete angular coverage, adequate transducer bandwidth, uniform sound speed, and negligible tissue interface reflections. However, variations in tissue sound speed introduce propagation distance errors and artifacts, while acoustic impedance mismatches increase scattering, leading to the limited-view problem and degrading image quality and depth resolution [55]. Although iterative reconstruction algorithms can mitigate these issues to some extent, they come with higher computational costs and require the selection of appropriate regularization techniques.

Despite significant engineering efforts to address PAI's technical challenges, most solutions rely on complex and expensive hardware, such as powerful light sources, two-dimensional ultrasound arrays, high-speed scanning mirrors, and time-consuming image reconstruction and processing, including iterative methods. These solutions often require balancing different imaging parameters, such as imaging speed versus field of view and spatial resolution versus penetration depth. Thus, PAI is in urgent need of innovative solutions to that address these challenges with a fresh perspective [56].

TABLE 6. A BRIEF SUMMARY OF DL-BASED RECONSTRUCTION APPROACHES FOR PACT.

DL methods	Models	Backbones
DL-based reconstruction During Pre-processing Stage	FC-DNN [66]	This study proposed a fully connected deep neural network (FC-DNN) to correct sonograms acquired by each transducer channel, broadening the bandwidth of received data and increasing the SNR of beamformed images.
DL-based reconstruction Within Direct-processing Stage	Res-Unet [69]	This study proposed a model that uses the entire raw signals as inputs with learned weights/filters to mitigate image reconstruction ill-posedness, and the Res-Unet successfully generated high-quality images with sharp edges and reduced artifacts
DL-based reconstruction Throughout Post-processing Stage	FD-UNet [70]	This study used the Fully Dense U-Net (FD-UNet) for post-processing reconstruction images, enhancing inter-layer feature information transmission and reducing redundant feature learning.
	PA-GAN [73]	This study removed artifacts due to limited view data using an unsupervised learning approach.
	PAT-AND [74]	This study designed an unsupervised learning Artifacts Disentangling Network (ADN) to address artifact issues in extremely sparse view scenarios.
	MDAEP [75]	This study combined Multi-Channel Denoising AutoEncoder Prior (MDAEP) with model iterations for high-resolution accelerated sparse reconstruction, integrating PAT's physical model with unsupervised multi-channel deep learning networks.
	DuDounet [71]	This study shared nearly identical texture information across dual domains but distinct artifact information, teaching the network how to differentiate these at the input level.
	NA Mechanism for Sparse PACT Reconstruction [77]	This study proposed a novel solution that employed the neighborhood attention (NA) mechanism for sparse PACT.

### IV. DEEP LEARNING-BASED RECONSTRUCTION IN PAI

DL has experienced unprecedented growth in recent years, driven by the availability of extensive datasets and advanced computational resources. It has become essential for various tasks including image classification, segmentation, reconstruction, super-resolution, and disease prediction. Moreover, DL has outperformed traditional algorithms in PAI reconstruction by generating high-quality images with elevated SNR, even under conditions of low pulse energy [57]. The integration of DL with PAI has facilitated significant advances in artifact removal, image denoising, and super-resolution [32], [51], [54]. Given its potential to efficiently reconstruct high-

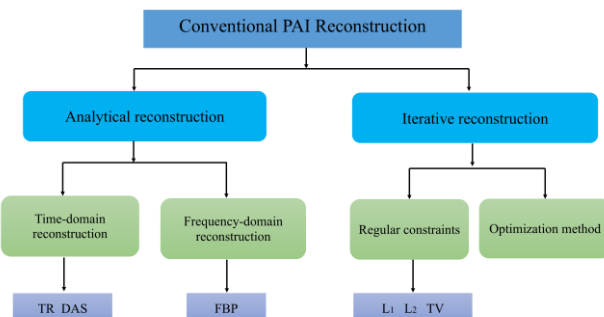


Fig. 5. Illustration of conventional PAI reconstruction methods.

quality images, DL-based image reconstruction aims to improve the quality of photoacoustic images under non-ideal conditions, while addressing challenges such as sparse sampling and finite-angle views, restricted bandwidths, heterogeneous media properties, finite aperture size of array elements, and insufficient laser power.

In 2017, Antholzer *et al.* [59] pioneered the application of convolutional neural networks (CNNs) for PAI reconstruction, which solved the complex inverse problem by learning complex mappings and optimal features to improve the reconstruction speed and image quality. In PACT, DL models yield high-fidelity three-dimensional imaging results [60]; in PAM, they enable recovery of high-contrast and high-resolution images from biological tissues [20]; whereas in PAE, they learn rich feature representations from limited datasets that improve clarity and detail within reconstructed images [13].

### 1) PACT Image Reconstruction

PACT is an emerging biomedical imaging modality that achieves high-contrast visualization of deep tissues by reconstructing initial pressure distribution from acoustic signals [36]. However, a primary challenge lies in obtaining high SNR images using cost-effective equipment. Sparse sampling of acoustic waves often results in suboptimal reconstructions accompanied by severe artifacts that obscure critical information [39], [42]. Recently developed numerous DL-based methodologies have been successfully implemented within PACT to enhance image reconstruction quality as outlined in Table 6 [61], [49], [50], [64], [65]. Subsequently, Fig. 6 illustrates the integration of acoustic inversion and deep learning in processing Radio Frequency (RF) data to generate reconstructed images, highlighting pre-processing pathways alongside post-processing strategies as well as direct processing approaches employed during analysis [10].

#### (1) DL-based reconstruction During Pre-processing Stage

Data preprocessing consists of applying neural networks to the raw data to optimize the initial dataset before traditional algorithms perform reconstruction, thereby mitigating interference due to limitations such as insufficient transducer bandwidth or limited-angle acquisitions. During signal pre-processing phases specifically designed neural networks are employed for processing photoacoustic sinograms which enhances both signal bandwidths along with resolution levels achieved during subsequent reconstructions. Photoacoustic signals captured at tissue boundaries are inherently band-limited phenomena. Gutta *et al.* [66] utilized fully connected

deep neural network (FC-DNN) aimed at correcting sonograms acquired via each transducer channel thereby broadening received data's effective bandwidth whilst increasing beamformed imagery's SNR by approximately 6 dB—a similar line-of-work was also reported by other researchers [67], [68].

#### (2) DL-based reconstruction Within Direct-processing Stage

Direct processing refers explicitly towards employing neural network architectures capable enough directly mapping relationships between incoming photoacoustic signals against their corresponding resultant photoacoustic image where entire processes remain dominated solely through these trained frameworks themselves. For instance, Feng *et al.* [69] proposed an end-to-end Res-UNet model facilitating direct generation outputting reconstructed PA-images based purely upon raw sensor inputs featuring telescopic symmetric expansion paths integrated throughout architecture design. Meanwhile, skip connections were added to learn the difference between input and output, and a residual learning mechanism was employed to prevent deep network degradation, successfully generating high-quality images with clear edges and fewer artifacts.

#### (3) DL-based reconstruction Throughout Post-processing Stage

Post-processing techniques aim primarily refining lower-quality outputs generated via conventional algorithms tackling issues stemming particularly due sparse sampling coupled together limited-angle acquisition scenarios encountered frequently. Antholzer *et al.* proposed using a U-Net network for postprocessing images reconstructed by the FBP algorithm to improve the quality of reconstructions under limited-angle conditions [59]. Guan *et al.* [70] presented Fully Dense U-Net (FD-UNet), an enhanced CNN architecture that uses dense connections to improve inter-layer feature transmission, making the model more compact and efficient. High-quality reconstructions under limited-angle sampling remain a challenge in PACT. Zhang *et al.* proposed Dual Domain Unet (DuDounet) with a specially designed Information Sharing Block (ISB), which can further share two domains' information and distinguish artifacts [71]. Lan *et al.*'s JEFF-Net leveraged a DL fusion framework with an innovative loss function to suppress artifacts [72]. Furthermore, unsupervised learning methods like PA-GAN [73] and PAT-AND [74] have been developed to overcome the lack of labeled data, with PAT-AND showing excellent performance under extremely sparse angular conditions.

Notably, physics-informed DL for photoacoustic tomography continues to receive extensive research attention. Song *et al.* proposed a novel fast sparse reconstruction strategy combining a multi-channel denoising autoencoder priors (MDAEP) with model-based iteration, integrating PACT's physical model with DL networks [75]. During the training phase, tri-channel images constructed from full-angle PACT data were used to learn high-dimensional priors via MDAEP networks. In the reconstruction stage, a conjugate gradient descent-based model iteration method was adopted to combine the learned high-dimensional priors with original data, constraining the network to generate high-quality PACT images. In 2024, Guo *et al.* introduced a new high-quality PACT strategy under limited-angle conditions based on a fractional diffusion model [76]. This method combines the physical model of PACT with a diffusion model, introducing high-dimensional

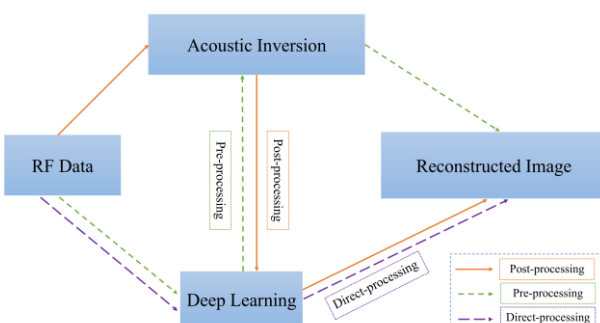


Fig. 6. Paradigm illustration using deep learning for PACT reconstruction.

priors learned by a deep network into the model-based iterative process. This approach significantly improves imaging quality, effectively addressing the degradation in image quality due to limited-angle sampling, and holds the potential for accelerating PACT imaging speed and expanding its application scope.

Sparse sampling is crucial for rapid data acquisition with low computation in PAI. However, reconstructing high-quality images from sparse data is challenging due to undersampling artifacts. Chan *et al.* [77] proposed a novel sparse PACT reconstruction method using a neighborhood attention (NA) mechanism, emphasizing local neighborhood information and spatial context. This work marks the first application of the sliding window attention mechanism to image restoration in PACT. Tong *et al.* [78] proposed a Feature Projection Network (FPNet) for directly reconstruction of photoacoustic images from sparse-sampled and limited-angle data, though it suffers from high computational resource consumption.

#### (4) DL-based reconstruction in the Hybrid-processing Stage

Lan *et al.*'s Y-Net was a hybrid DL framework that combines direct reconstruction with postprocessing to extract information from raw data and preliminary reconstructed images[79]. Inspired by the U-Net network, Y-Net reconstructs the initial PA pressure distribution by optimizing both raw data and beamformed images using two encoder paths and one decoder path.

#### 2) PAM Image Reconstruction

In PACT and PAM, the application of DL exhibits notable distinctions. Since PAM does not require inverse reconstruction, DL models can directly map input signals to output images, thereby enhancing image quality [3], [59]. Consequently, DL is particularly apt for addressing numerous challenges in PAM, such as improving ill-posed reconstructions, removing artifacts, denoising channel data, enhancing spatial resolution, and up-sampling sparse scan input data. As an efficient GPU-accelerated method, DL can robustly approximate nonlinear spatial mappings within a reasonable optimization timeframe. Existing image reconstruction algorithms, through continuous refinement and development, have achieved significant outcomes. This section will elaborate on the impact of current deep learning models on the final performance of photoacoustic images, specifically focusing on their roles in enhancing resolution, reducing noise, and improving imaging depth, all within the context of PAM reconstruction.

#### (1) Deep Learning for Resolution Enhancement in PAM Reconstruction

Spatial resolution is a critical metric for assessing the performance of photoacoustic images, which is affected not only by the hardware system but also by the accuracy of the reconstruction algorithm. When PAM technology speed up imaging by decreasing the spatial sampling density and increasing the scanning step size, they also lead to image resolution degradation and spatial aliasing. DL has been used to reduce the laser pulse energy and improve the undersampling of PAM.

Recently, researchers have developed a method using a non-pretrained Deep Iterative Prior (DIP) model to enhance undersampled PAM images and speed up imaging [80]. The DIP model iteratively optimizes fully sampled images from undersampled data using a known downsampling mask, enhancing generalization without paired training. Tested on

TABLE 7. A BRIEF SUMMARY OF DL-BASED RECONSTRUCTION APPROACHES FOR PAM.

Aims	Models	Backbones
Deep Learning-Driven Resolution Enhancement in PAM Reconstruction	DIP [80]	This study proposed a DIP model that iteratively optimizes a fully sampled image to approximate the undersampled image using a known downsampling mask, enhancing generalization capabilities.
	SRResNet [81]	This study proposed a deep learning-based method to reconstruct undersampled PAM data in 3D, enhancing imaging speed 80-fold and reducing data volume 800-fold, with improvements to the SRResNet framework for better applicability.
	PADA U-Net [83]	This study proposed the Photoacoustic Dense Attention U-Net (PADA U-Net) model to reconstruct fully scanned images from undersampled ones, breaking the trade-off between imaging speed and spatial resolution.
	BRn-ResNet [84]	This study proposed BRn-ResNet, which uses batch renormalization and residual networks to enhance training stability and eliminate subsampling artifacts in photoacoustic imaging, addressing data insufficiency and training interference by processing inaccurate sparse images and removing abnormalities.
	Mean-reverting diffusion model [85]	This study proposed a novel mean-reverting diffusion model-aided method to balance imaging depth and lateral resolution in AR-PAM and OR-PAM, transitioning lateral resolution to optical levels while maintaining deep penetration, by modeling the degradation process and iteratively executing a reverse-time SDE to recover high-quality images from noise.
	MT-RDN [88]	This study proposed the Multi-Task Residual Dense Network (MT-RDN), which integrates multi-supervision learning, dual-channel sample acquisition, and rational weight distribution.
	UPAMNet [90]	This study proposed an end-to-end network named UPAMNet, which incorporates built-in attention blocks and both pixel-level and perception-level priors through semantic segmentation and deep features, achieving high-fidelity PAM image super-resolution and denoising.
	PnP Prior [93]	This study proposed a deep CNN-based prior integrated into a model-based reconstruction framework for photoacoustic microscopy, validated through in vivo AR-PAM experiments, using FFDNet for adaptive AWGN denoising, enhancing image contrast, resolution, and detail.
	ResUnet-AG [94]	This study proposed a two-stage deep learning reconstruction strategy for AR-PAM using a residual U-Net with attention gates to adaptively recover high-resolution photoacoustic images at different out-of-focus depths.
	DiffPam [95]	This study proposed a novel method using a pre-trained diffusion model to reconstruct degraded PAM images, simplifying training and enabling adaptable operations such as super-resolution, denoising, or inpainting.

mouse brain vasculature and bio-printed gel images, it outperformed interpolation methods and pretrained DL models without needing prior training data, marking its first application in PAM.

Seong *et al.* [81] developed a DL-based method for 3D volumetric reconstruction in PAM, reducing imaging time and data volume by fully reconstructing undersampled datasets. They adapted SRResNet and validated its performance to realize the first DL-based 3D reconstruction of undersampled PAM data.

Li *et al.* [82] introduced PSAD-UNet, a polarized self-attention dense U-Net, which enhances transcranial PAI by mitigating the impact of bone plates. This model demonstrates broad application potential in both preclinical and clinical settings. Similarly, Wang *et al.* [83] proposed the Photoacoustic Dense Attention U-Net (PADA U-Net) to reconstruct full-scanning images from undersampled data, breaking the trade-off between imaging speed and spatial resolution. Shahid *et al.* [84] addressed the undersampling problem of sparse data by proposing a Batch Renormalization Aggregated Residual Network (BRn-ResNet). This network enhances U-Net by introducing residual blocks to improve training stability and eliminate artifacts caused by sparse data, achieving an SSIM of 0.97.

Cao *et al.* [85] proposed a mean-reverting diffusion model for AR-PAM, using iterative reverse-time SDE to balance imaging depth and lateral resolution. This method enhances PAM imaging quality and broadens its applicability by improving lateral resolution without sacrificing depth. Le *et al.* [86] demonstrated a computational strategy using two GANs to perform semi/unsupervised high-resolution and sensitive reconstruction in AR-PAM. This approach maintains imaging capability at enhanced depths. Similarly, Cheng *et al.* [87] used deep learning-enabled image transformation to improve deep penetration OR-PAM performance.

Zhao *et al.* [88] proposed a multi-task residual dense network (MT-RDN) to improve the image quality in traditional OR-PAM systems at ultra-low laser doses. This method enhanced image quality through multi-supervision learning, dual-channel sample acquisition, and densely connected layers for local feature fusion, providing richer reconstruction details.

## (2) Deep Learning for Image Denoising in PAM Reconstruction

Noise severely affects photoacoustic image reconstruction and causes a large number of artifacts. Sources of noise include hardware limitations as well as phase mismatch due to inhomogeneous sound velocity and scattering in the target tissue, which hinders accurate phase representation. Zhou *et al.* [89] proposed an optoacoustic signal denoising method combining empirical mode decomposition (EMD) and conditional mutual information. EMD adaptively decomposes the noisy photoacoustic signals into multiple intrinsic mode functions (IMFs), and utilizes the conditional mutual information to denoising.

Liu *et al.* [90] proposed a Unified Photoacoustic Microscopy Image Reconstruction Network (UPAMNet), which combines DL with image prior knowledge to address super-resolution and denoising in PAM images. Using three attention-based modules and mixed training constraints, UPAMNet improved PSNR by

0.59 dB and 1.37 dB for 1/4 and 1/16 undersampled images, respectively, and enhanced denoising by 3.9 dB.

In photoacoustic imaging, ultrasound attenuation due to absorption and scattering within the tissues, phase deviation caused by variations in sound speed, and signal waveform broadening associated with acoustic attenuation can all degrade spatial resolution. To address this issue, He *et al.* [91] proposed an attention-enhanced GAN that uses an improved U-net generator to remove noise from PAM images.

The spatial resolution of AR-PAM imaging is relatively low, hindering its widespread application [92]. Previous models or learning algorithms either required complex priors or lacked interpretability and flexibility, failing to adapt to different degradation models. To address this, Zhang *et al.* [93] proposed a model that combines a deep CNN with a model to adaptively handle various degradation functions in AR-PAM image enhancement. The algorithm learns vascular image statistics as a PnP prior, enhancing both simulated and in vivo images with significant improvements in PSNR, SSIM, SNR, and CNR, demonstrating its interpretability, flexibility, and broad applicability.

## (3) Deep Learning for Imaging Depth Enhancement in PAM Reconstruction

In clinical applications, the demand for imaging and analyzing deep tissues makes imaging depth a critical focus. Neural networks play a pivotal role in advancing this aspect.

Li *et al.* proposed an end-to-end universal fusion framework based on CNNs. This framework leverages convolutional layers to extract useful information from photoacoustic images and integrates features according to specific tasks, transforming images with low structural information into those with high structural information. This renders photoacoustic images of deeper tissues usable, thereby enhancing imaging depth.

TABLE 8. A BRIEF SUMMARY OF DL-BASED RECONSTRUCTION APPROACHES FOR PAE.

Models	Backbones
Focus U-Net [97]	This study incorporated several architectural modifications into the Focus U-Net, including the addition of short-range skip connections and deep supervision.
Wavelet Transform and Guided Filter Decomposition-Based Fusion Approach [98]	This study proposed an approach to improve the visual quality of endoscopic images by using artificially generated sub-images and image fusion techniques
Contrast Limited Adaptive Histogram Equalization (CLAHE) [99]	This study proposed a method to enhance endoscopic images by generating three complementary sub-images using Contrast Limited Adaptive Histogram Equalization (CLAHE), image brightening, and detail enhancement.
Approximate Gaussian acoustic field [100]	This study proposed a new photoacoustic/ultrasound endoscopic imaging reconstruction algorithm based on the approximate Gaussian acoustic field which significantly improves the resolution and signal-to-noise ratio (SNR) of the out-of-focus region.
Improved back-projection (IPB) algorithm [101]	This study developed an improved back-projection (IPB) algorithm for focused detection over centimeter-scale imaging depth and a deep-learning-based algorithm to remove electrical noise.

To address the poor reconstruction performance of traditional AR-PAM systems in deep-focus or out-of-focus regions. Meng *et al.* developed a Residual U-Net network architecture with an attention mechanism, named ResUnet-AG [94]. This network ensures that background and other noise information are ignored during learning through the attention mechanism, thereby improving the imaging effect in deeper tissue areas. The network extended the depth of field of AR-PAM from 1 to 3 millimeters, significantly enhancing the imaging depth.

Beyond neural network methods, a pyramid structure fusion concept capable of dramatically increasing imaging depth has been proposed in recent years. Improving the speed of PAI has always been a key concern for researchers. In PAM, the limitation imposed by the laser pulse repetition rate on speed has highlighted the potential role of computational methods in accelerating PAM imaging. Loc *et al.* proposed a novel and highly adaptive DiffPam algorithm that leverages diffusion models to expedite PAI [95]. Research findings indicate that DiffPam achieves performance comparable to specialized U-Net models without requiring large datasets or training DL models. Additionally, the study demonstrated the efficacy of shortening the diffusion process in reducing computational time without compromising accuracy. Table 7 summarizes the PAM reconstruction approaches.

### 3) PAE Image Reconstruction

Endoscopy is an indispensable tool for the diagnosis of internal organ diseases in the human body. However, images obtained directly through endoscopy are often insufficient to differentiate microvessels or identify lesions from the tissue background due to the internal environment and imaging conditions [13]. PAE faces the same challenges posed by limited fields of view and a complex *in vivo* environment. In practice, factors such as blood, illumination variations, specular reflections, and smoke introduce noise, degrading image quality, especially in occluded regions. Therefore, it is crucial to improve the quality of endoscopic images by enhancing details, improving contrast, adjusting brightness and removing specular reflection highlights [96].

Yeung introduced Focus U-Net [97], a dual attention-gated deep neural network that integrates spatial and channel-based attention mechanisms into a single Focus Gate module, promoting selective learning of polyp features. The network includes short-range skip connections, deep supervision, and a Hybrid Focal Loss to address class imbalance, and it holds potential for noninvasive colorectal cancer screening and other biomedical image segmentation tasks.

In clinical surgery, the quality of endoscopic images is degraded by noise. Zhang *et al.* [98] proposed an improved weighted guided filtering model to enhance vessel details and contours in endoscopic images. The model includes detail enhancement, contrast enhancement, brightness enhancement, and highlight area removal, effectively suppressing noise while maintaining the original image structure, thus improving tissue vessel details and providing guidelines for endoscopy device development.

On this basis, Moghtaderi *et al.* [99] introduced a method to enhance endoscopic images by generating three complementary sub-images using Contrast Limited Adaptive Histogram Equalization (CLAHE), image brightening, and detail enhancement. These sub-images are then decomposed using a

multi-level wavelet transform and guided filters, followed by weighted fusion to produce the final enhanced image, making it suitable for low-light image enhancement applications.

Improving the resolution and SNR of the defocused region is of great significance for the design of acoustically focused ultrasound/photoacoustic endoscopy system. Wang *et al.* [100] proposed a new photoacoustic/ultrasound endoscopic imaging reconstruction algorithm based on an approximate Gaussian acoustic field, which improves the resolution and SNR of the out-of-focus region. Tested in a chicken breast phantom and a rabbit rectal endoscopy experiment, the algorithm demonstrated higher-quality imaging, enabling fast dynamic focusing and enhancing overall imaging quality.

Due to many technical difficulties, the study of molecular photoacoustic endoscopic (PAE) imaging in deep tissues is limited. Xiao *et al.* [101] developed an improved back-projection (IBP) algorithm for focused detection over centimeter-scale imaging depth and a deep-learning-based algorithm to remove electrical noise from the step motor, reducing scanning time and promoting the development of high-penetration molecular PAE.

## V. DEEP LEARNING-BASED QUANTITATIVE ANALYSIS IN PHOTOACOUSTIC IMAGING

PAI can provide structural, functional, molecular, and kinetic information using both endogenous contrast agents (e.g., hemoglobin, lipid, melanin, water) and various exogenous contrast agents. A notable feature of PAI is its ability to discriminate between deoxy-hemoglobin (Hb) and oxy-hemoglobin (HbO<sub>2</sub>), allowing the measurement of oxygen saturation (sO<sub>2</sub>) in blood vessels, which is crucial for detecting physiological states such as ischemia, hypoxia, or hypoxemia [102]. Additionally, PAI exploits the optical absorption properties of melanin for imaging melanoma, pigmented lesions, and hair follicles. Clinically relevant, FDA-approved contrast agents like ICG and methylene blue, which have strong photoacoustic properties, are valuable in PAI applications [20]. Therefore, quantitative analysis in PAI is essential and involves two critical aspects: optical fluence compensation and spectral unmixing [103].

### A. Optical Fluence Compensation

The accuracy and clinical effectiveness of quantitative PAI (qPAI) are influenced by the spatial distribution of optical fluence, which varies with depth and wavelength. Optical fluence compensation corrects image distortions caused by inhomogeneous light distribution, enhancing the accuracy of physiological parameters like hemoglobin concentration and oxygen saturation. DL models can learn complex feature representations from raw data and train networks to estimate and compensate for fluence differences due to variations in tissue optical properties. This approach can automatically and efficiently handle the compensation task, thereby improving the quality of the image reconstruction. To address this, compensation methods include model-based methods, iterative compensation methods, multimodal approaches, deep learning-based methods, and other fluence compensation techniques [103].

### 1) Model-based Methods

Several models of light transport are used to determine optical fluence, including the photon diffusion equation (PDE), Monte Carlo (MC) models based on the radiative transfer equation (RTE) [104], and the diffusion dipole model (DDM) [105]. PDE is suitable for macroscopic descriptions, as demonstrated by Zhao *et al.* with FEA-generated fluence maps [106]. MC simulations, employed by Kirillin *et al.* [107] and Hirasawa *et al.* [108], model individual photons and mitigate spectral coloring. Ranasinghesagara *et al.* [109] used multi-illumination PA microscopy (MI-PAM) to measure optical properties, which were then input into an MC model to calculate fluence.

### 2) Iterative Compensation Methods

Iterative fluence compensation refines fluence distribution through an optimization process, starting with an initial estimate and updating it iteratively to match observed photoacoustic signals until convergence. This method does not require prior knowledge of optical parameters, making it more robust and accurate than model-based methods, which can introduce biases with inaccurate parameters. Iterative algorithms adapt well to complex conditions but demand high computational resources, especially with 3D data or MC models [110]. While minimizing iterations is ideal, achieving higher accuracy often necessitates more iterations or a more sophisticated algorithm, presenting a trade-off between accuracy and computational demands.

### 3) Multimodal Approaches

USI in combination with PAI can provide dual-modality imaging, using structural information to improve fluence maps and photoacoustic image quality [111]. However, USI requires time-consuming segmentation and identification, which may need experienced clinicians. AI-based segmentation can reduce the time cost, but processing ultrasound images, especially in 3D, demands significant computational resources. Diffuse optical tomography (DOT) also reconstructs 3D maps of tissue optical properties to enhance fluence accuracy in deep tissue PAI. While DOT shares benefits with USI, it similarly requires additional optical equipment and extensive processing, increasing computational demands.

### 4) Deep Learning-based Methods

A relatively new method for optical fluence compensation in photoacoustic images is deep learning. For instance, Yang *et al.* [102] used a deep residual recurrent neural network (DR2U-Net) to estimate sO<sub>2</sub> levels in photoacoustic images. However, the accuracy and generalizability of DL models depend on having sufficient photoacoustic data. Training these models requires substantial computational resources and time, and complex architectures can lead to longer processing times.

### 5) Other Fluence Compensation Methods

Another method used to compensate for optical fluence variations is wavefront shaping. In a study by Caravaca-Aguirre *et al.*, a spatial light modulator (SLM) was used to modulate the wavefront of a 532 nm laser beam before it was focused onto two capillary tubes behind a glass diffuser [112]. To improve the measurement of sO<sub>2</sub> using photoacoustic images, Fadhel *et al.* developed a fluence matching algorithm to correct errors in raw photoacoustic images arising from wavelength-dependent fluence variations [113].

### B. Spectral Unmixing

Spectral unmixing is a technique that decomposes signals from multiple absorbers within a pixel, facilitating to quantify individual chromophores such as oxy- and deoxyhemoglobin, lipid content, and melanin. Photoacoustic (PA) data is typically acquired across several wavelengths, resulting in multispectral images that encapsulate mixed information from various chromophores [114], [115]. Applying deep learning for spectral unmixing can enhance the separation of different absorbers from these mixed signals. By training deep learning models to identify and isolate the spectral signatures of diverse absorptive substances, more accurate quantitative analyses can be achieved. Despite the complexity of tissues composition, spectral unmixing techniques have proven effective in distinguishing these chromophores. As its name suggests, the spectral unmixing technique aims to decode mixed pixels into a set of end members by determining the contribution of each end member to the observed spectrum at each pixel location [116].

#### 1) Linear Spectral Fitting

Traditional approaches to solving the spectral unmixing problem include applying a linear regression algorithm assuming that each pixel in the photoacoustic image represents a linear combination of absorption and concentration of different chromophores, i.e., the linear mixing model (LMM) [117]. Feng *et al.* detected collagen as a biomarker for bone health assessment by multi-wavelength PA (MWPA) [118]. Conventional linear spectral fitting partially solves the problem but is limited by known absorption spectra and spectral coloring effects in complex tissues [115].

#### 2) Statistical Detection Method

Statistical detection methods focus on identifying specific target spectrum without requiring explicit knowledge of background absorption spectra. This makes them ideal for detecting molecules with known spectra, such as exogenous nanoparticles, reporter genes, and oxy- and deoxy-hemoglobin. For example, Tzoumas *et al.* [119] introduced eigenspectra multispectral optoacoustic tomography (eMSOT) to estimate oxygen saturation (sO<sub>2</sub>) levels in vivo. These methods typically rely on large datasets, which can increase computational demands and pose challenges, especially in the case of in vivo measurements.

#### 3) Blind Source Unmixing

The exploration of various blind source unmixing algorithms holds promise in mitigating the challenges of linear spectral unmixing and enhancing the precision of qPAI. More importantly, blind source unmixing is a method capable of separating images without relying on a prior knowledge of spectral signature or fluence distribution. This technique possesses the capability to recover unknown source "signals" solely based on the understanding of observed mixtures of these signals within an image, which is more suitable to study complex biological tissues [120].

#### 4) Learning-based Spectral Unmixing

Kirchner *et al.* developed CE-qPAI using Monte Carlo simulations and random forests to enhance spectral unmixing [121]. Cai *et al.* introduced an end-to-end ResU-net approach for accurate quantitative imaging in simulations. Gröhl's team used LSD with a neural network to improve oxygenation

estimation accuracy [122]. Olefir *et al.* [123] enhanced MSOT with DL-eMSOT, achieving superior performance using synthetic data.

In addressing the challenges of qPAI, it is essential to account for spatial variations in optical fluence to derive accurate absorption maps (shown in Fig. 7). Strategies include model-based methods, iterative compensation, multimodal approaches, and deep-learning techniques. Robust spectral unmixing is also critical for accurately obtaining physiological and biochemical information at depth. Recent advancements such as linear spectral fitting, statistical detection methods, blind source unmixing, and learning-based approaches have significantly improved the decoding of mixed pixel information into distinct chromophores. Notably, the challenges in qPAI are often interconnected due to the hybrid nature of optical absorption and acoustic detection; recognizing this interdependence is beneficial for developing effective strategies to enhance qPAI's reliability and applicability across various biomedical contexts.

## VI. FUTURE WORK

The clinical applications of PAI have been extensively investigated, with the International Photoacoustic Standardization Consortium advocating for the standardization of data management, hardware testing, and clinical utilization. Despite receiving approvals from FDA and CE, as well as being incorporated into the DICOM standard [7], it still faces several challenges including limited optical penetration depth, high equipment costs, and concerns regarding patient safety [124]. Ongoing advancements in hardware and software technologies, coupled with the integration of artificial intelligence (AI) to enhance imaging quality, depth resolution, and acquisition speed are anticipated to mitigate these issues. Consequently, future research should concentrate on the following critical areas.

### A. Single Image Super-Resolution in PAI

Providing high-resolution photoacoustic images is essential for clinical applications and image analysis; however, hardware limitations often necessitate trade-offs in scan time, SNR, and spatial coverage. DL-based super-resolution techniques, extensively researched in other modalities, enhance both the efficiency and accuracy of PAI reconstruction processes. These methodologies leverage innovative residual architectures alongside recursive learning mechanisms, attention frameworks, efficient feature distillation modules, and multi-scale feature extraction strategies to optimize gradient flow while enhancing model stability and detailed information capture. Combining dense connections and feedback mechanisms leverages prior information for self-correction, contributing to stable iterative optimization and accelerated model convergence, thus improving reconstruction fidelity.

Implementing SISR techniques within PAE imaging enhances diagnostic value along with analytical precision without necessitating costly hardware upgrades. By employing advanced deep learning models tailored for SISR tasks higher-fidelity reconstructions can be achieved enabling clearer visualization of anatomical structures as well as potential pathologies present therein. Since Dong *et al.*'s pioneering work in 2014 [125], optimized models such as SRCNN [126],

SRGAN [127], CAMixerSR [128], and CoSeR [129] have emerged showcasing significant progress within super-resolution technology domain specifically applicable across medical imaging contexts. Furthermore deep-structured networks like VDSR [130], DRRN [131], RFDN [132] combined with innovative frameworks exemplified by Deep Multi-Scale Network (DMSN) [133] have further enhanced quality metrics associated with existing SR methods utilized throughout healthcare settings.

### B. Physics-Informed Reconstruction in PAI

In relation to PAI itself directly mapping photoacoustic signals onto photoacoustic imaging via deep learning approaches presents considerable challenges particularly when addressing incomplete projection datasets; additionally, this methodology typically demands extensive training datasets, resulting in elevated computational expenses incurred during processing phases. To counteract these obstacles physics-informed deep learning paradigms specific towards PAI have surfaced integrating rapid physical modeling simulations alongside AI-driven inverse problem-solving techniques aimed at achieving high-quality reconstructions whilst concurrently reducing overall computational times required. Specifically, incorporating physical constraints along with prior knowledge derived from established physical models has shown substantial improvements in the performance robustness of contemporary DL architectures. Current research initiatives focusing upon amalgamating traditional physics-based modeling approaches together with modern DL methodologies—as demonstrated through implementations such as PAT-MDAE [75] and the physics-driven DL-based filtered back projection (dFBP) framework [134], illustrate promising outcomes. This hybrid strategy leverages the strengths inherent in both physics-oriented frameworks and data-centric deep learning (DL) solutions, presenting a compelling avenue forward to enhance the efficacy of diverse biomedical applications involving PAI.

### C. Deep Learning-Based Multimodal Fusion in PAI

In multimodal imaging systems, the fusion of PAI with OCT, ultrasound, and other modalities enhances imaging depth and spatial resolution, providing comprehensive information about biological tissues [135]. Multimodal image-guided surgical navigation, combining techniques like endoscopy, ultrasound,

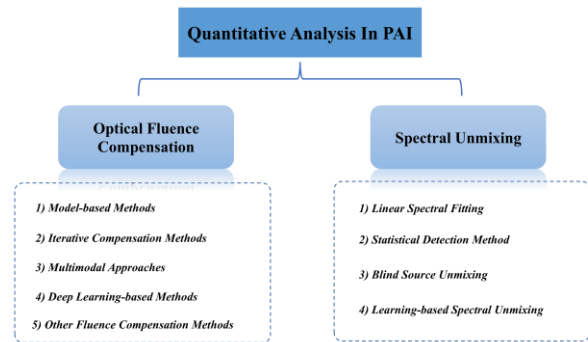


Fig. 7. Overview of quantitative analysis of PAI.

and fluorescence, has improved the visualization and spatial identification of critical structures, aiding minimally invasive procedures in neurosurgery, crano-maxillofacial correction,

orthopedics, biopsies, and vascular interventions. Key technologies that facilitate these improvements include multimodal image segmentation, surgical planning, position calibration, image registration, and multi-source information fusion. Recent advancements in image fusion techniques, such as GANMcC [136], utilize GANs alongside Transformers to effectively integrate gradient and intensity information. Duan *et al.* [137] proposed a novel architecture that integrates both Transformer and CNN elements, featuring global and local branches within the encoder module. Furthermore, the combination of photoacoustic/ultrasound systems with methods like diffuse optical tomography and MRI enhances disease monitoring and diagnosis; this is particularly beneficial for brain imaging aimed at obtaining functional and molecular insights through MRI. Anatomical data derived from ultrasound improves the lateral resolution of PAI systems, enabling detailed visualization of cerebral vasculature [138]. Additionally, it is crucial to evaluate these fusion technologies in clinical settings to ensure their continued advancement [139].

#### D. Quantitative Analysis in PAI

Future research at qPAI aims to enhance luminous flux modeling for precise tissue absorption coefficient reconstructions, improve spectral unmixing with advanced methods, and develop unsupervised super-resolution models to address data scarcity. Efforts will also be made to create compact and efficient network models, innovate evaluation metrics aligned with human perception, and deepen the theoretical understanding of DL for better reliability and interpretability. Advancements in reconstruction techniques will address limited view and acoustic heterogeneity while integrating deep learning for real-time reconstruction. Combining qPAI with other imaging modalities will improve resolution and contrast. Establishing efficacy and safety through clinical trials, investigating new contrast agents, designing portable and affordable systems, and extending qPAI to functional and molecular imaging to quantify physiological parameters will further advance its application in biomedical research and clinical diagnosis [140].

## VII. CONCLUSION

PAI has emerged as a formidable technique for high-resolution visualization of optical contrast in biological tissues, effectively overcoming the limitations of traditional optical imaging methods. Over the past decade, an extensive body of research has substantiated the advantages of this technique in disease screening, diagnosis, and monitoring across a range of organs. This review commences with an exposition of the fundamental principles underlying PAI and its superiority over OCT and US. Thereafter, it examines the limitations of conventional approaches and the critical role of deep learning in advancing PACT, PAM, and PAE. The implementation of AI-drive techniques is paramount for mitigating image degradation resulting from limited spatial sampling in PAI. These techniques, which are tailored to accommodate a variety of system configurations, sampling conditions, and imaging targets, have the capacity to markedly reduce artefacts, enhance anatomical visibility, improve wave source localization, and enable precise quantitative assessments. It is crucial to address

spatial variations in optical fluence in order to accurately derive absorption maps in tissue imaging. Similarly, robust spectral unmixing is vital for obtaining precise physiological and biochemical data at depth. Overcoming these challenges will be pivotal to the broader clinical application of PAI. The review concludes with an examination of prospective avenues for research in PAI, including single-image super-resolution, physics-informed deep learning, multimodal image fusion, and quantitative analysis. It underscores the transformative impact of deep learning on the ongoing evolution within this field.

## VIII. COMPETING INTERESTS

The authors declare no competing interests.

## REFERENCES

- [1] A. A. Oraevsky *et al.*, “Laser-based optoacoustic imaging in biological tissues,” in *Laser-Tissue Interaction V; and Ultraviolet Radiation Hazards*, Los Angeles, United States: SPIE, Aug. 1994, p. 16.
- [2] T. P. Matthews and M. A. Anastasio, “Joint reconstruction of the initial pressure and speed of sound distributions from combined photoacoustic and ultrasound tomography measurements,” *Inverse Problems*, vol. 33, no. 12, p. 124002, Dec. 2017.
- [3] L. V. Wang, “Tutorial on Photoacoustic Microscopy and Computed Tomography,” *IEEE J. Select. Topics Quantum Electron.*, vol. 14, no. 1, pp. 171–179, 2008.
- [4] J. Poudel *et al.*, “A survey of computational frameworks for solving the acoustic inverse problem in three-dimensional photoacoustic computed tomography,” *Phys. Med. Biol.*, vol. 64, no. 14, July. 2019.
- [5] B. Ning *et al.*, “Ultrasound-aided Multi-parametric Photoacoustic Microscopy of the Mouse Brain,” *Sci Rep*, vol. 5, no. 1, p. 18775, Dec. 2015.
- [6] S. Zackrisson *et al.*, “Light In and Sound Out: Emerging Translational Strategies for Photoacoustic Imaging,” *Cancer Research*, vol. 74, no. 4, pp. 979–1004, Feb. 2014.
- [7] J. Park *et al.*, “Clinical translation of photoacoustic imaging,” *Nat Rev Bioeng*, Sep. 2024.
- [8] S. Park *et al.*, “Contrast-enhanced dual mode imaging: photoacoustic imaging plus more,” *Biomed. Eng. Lett.*, vol. 7, no. 2, pp. 121–133, May 2017.
- [9] P. Rajendran *et al.*, “Photoacoustic imaging aided with deep learning: a review,” *Biomed. Eng. Lett.*, vol. 12, no. 2, pp. 155–173, May 2022.
- [10] A. DiSpirito *et al.*, “Sounding out the hidden data: A concise review of deep learning in photoacoustic imaging,” *Exp Biol Med (Maywood)*, vol. 246, no. 12, pp. 1355–1367, Jun. 2021.
- [11] J. Park *et al.*, “Quadruple ultrasound, photoacoustic, optical coherence, and fluorescence fusion imaging with a transparent ultrasound transducer,” *Proc. Natl. Acad. Sci. U.S.A.*, vol. 118, no. 11, p. e1920879118, Mar. 2021.
- [12] R. R. Gharieb, Ed., ‘Photoacoustic Imaging - Principles, Advances and Applications’. IntechOpen, May 06, 2020, 124.
- [13] H. Guo *et al.*, “Photoacoustic endoscopy: A progress review,” *Journal of Biophotonics*, vol. 13, no. 12, p. e202000217, Dec. 2020.
- [14] B. Cox *et al.*, “Quantitative spectroscopic photoacoustic imaging: a review,” *J. Biomed. Opt.*, vol. 17, no. 6, p. 061202, 2012.
- [15] J. Xia *et al.*, “PHOTOACOUSTIC TOMOGRAPHY: PRINCIPLES AND ADVANCES (Invited Review),” *PIER*, vol. 147, pp. 1–22, 2014.
- [16] S. Park *et al.*, “Real-time Triple-modal Photoacoustic, Ultrasound, and Magnetic Resonance Fusion Imaging of Humans,” *IEEE Trans. Med. Imaging*, vol. 36, no. 9, pp. 1912–1921, Sep. 2017.
- [17] S. Mallidi *et al.*, “Photoacoustic imaging in cancer detection, diagnosis, and treatment guidance,” *Trends in Biotechnology*, vol. 29, no. 5, pp. 213–221, May 2011.
- [18] P. Beard, “Biomedical photoacoustic imaging,” *Interface Focus.*, vol. 1, no. 4, pp. 602–631, Aug. 2011.
- [19] Y. Yu *et al.*, “Simultaneous photoacoustic and ultrasound imaging: A review,” *Ultrasonics*, vol. 139, p. 107277, Apr. 2024.
- [20] L. V. Wang, “Multiscale photoacoustic microscopy and computed tomography,” *Nature Photon*, vol. 3, no. 9, pp. 503–509, Sep. 2009.

[21] C. Liu *et al.*, "The integrated high-resolution reflection-mode photoacoustic and fluorescence confocal microscopy," *Photoacoustics*, vol. 14, pp. 12–18, Jun. 2019.

[22] A. B. E. Attia *et al.*, "A review of clinical photoacoustic imaging: Current and future trends," *Photoacoustics*, vol. 16, p. 100144, Dec. 2019.

[23] M. Omar *et al.*, "Optoacoustic mesoscopy for biomedicine," *Nat Biomed Eng*, vol. 3, no. 5, pp. 354–370, Apr. 2019.

[24] M. Moothanchery and M. Pramanik, "Performance Characterization of a Switchable Acoustic Resolution and Optical Resolution Photoacoustic Microscopy System," *Sensors*, vol. 17, no. 2, p. 357, Feb. 2017.

[25] L. Lin and L. V. Wang, "The emerging role of photoacoustic imaging in clinical oncology," *Nat Rev Clin Oncol*, vol. 19, no. 6, pp. 365–384, Jun. 2022.

[26] L. Li and L. V. Wang, "Recent Advances in Photoacoustic Tomography," *BME Front*, vol. 2021, p. 9823268, Jan. 2021.

[27] S. Na and L. V. Wang, "Photoacoustic computed tomography for functional human brain imaging [Invited]," *Biomed. Opt. Express*, vol. 12, no. 7, p. 4056, Jul. 2021.

[28] A. Q. Bauer *et al.*, "Quantitative photoacoustic imaging: correcting for heterogeneous light fluence distributions using diffuse optical tomography," *J. Biomed. Opt.*, vol. 16, no. 9, p. 096016, 2011.

[29] C. Tian *et al.*, "Spatial resolution in photoacoustic computed tomography," *Rep. Prog. Phys.*, vol. 84, no. 3, p. 036701, Mar. 2021.

[30] M. Jeon and C. Kim, "Multimodal Photoacoustic Tomography," *IEEE Trans. Multimedia*, vol. 15, no. 5, pp. 975–982, Aug. 2013.

[31] S. Jeon *et al.*, "Review on practical photoacoustic microscopy," *Photoacoustics*, vol. 15, p. 100141, Sep. 2019.

[32] T. Vu *et al.*, "A generative adversarial network for artifact removal in photoacoustic computed tomography with a linear-array transducer," *Exp Biol Med (Maywood)*, vol. 245, no. 7, pp. 597–605, Apr. 2020.

[33] I. Steinberg *et al.*, "Photoacoustic clinical imaging," *Photoacoustics*, vol. 14, pp. 77–98, Jun. 2019.

[34] P. Rajendran and M. Pramanik, "Deep learning approach to improve tangential resolution in photoacoustic tomography," *Biomed. Opt. Express*, vol. 11, no. 12, p. 7311, Dec. 2020.

[35] S. Zhang *et al.*, "Challenges and advances in two-dimensional photoacoustic computed tomography: a review," *J. Biomed. Opt.*, vol. 29, no. 07, Jul. 2024.

[36] C. Tian, M. Pei *et al.*, "Impact of System Factors on the Performance of Photoacoustic Tomography Scanners," *Phys. Rev. Applied*, vol. 13, no. 1, p. 014001, Jan. 2020.

[37] J. Yao and L. V. Wang, "Perspective on fast-evolving photoacoustic tomography," *J. Biomed. Opt.*, vol. 26, no. 06, Jun. 2021.

[38] Y. Zhou *et al.*, "Tutorial on photoacoustic tomography," *J. Biomed. Opt.*, vol. 21, no. 6, p. 061007, Apr. 2016.

[39] Z. Balci and A. Mert, "Enhanced photoacoustic signal processing using empirical mode decomposition and machine learning," *Nondestructive Testing and Evaluation*, pp. 1–13, Jun. 2024.

[40] J. Yao and L. V. Wang, "Photoacoustic microscopy," *Laser & Photonics Reviews*, vol. 7, no. 5, pp. 758–778, Sep. 2013.

[41] K. M. Kempksi *et al.*, "Application of the generalized contrast-to-noise ratio to assess photoacoustic image quality," *Biomed. Opt. Express*, vol. 11, no. 7, p. 3684, Jul. 2020.

[42] Q. Chen *et al.*, "Progress of clinical translation of handheld and semi-handheld photoacoustic imaging," *Photoacoustics*, vol. 22, p. 100264, Jun. 2021.

[43] K.-T. Hsu *et al.*, "Comparing Deep Learning Frameworks for Photoacoustic Tomography Image Reconstruction," *Photoacoustics*, vol. 23, p. 100271, Sep. 2021.

[44] T.-J. Yoon, "Recent advances in photoacoustic endoscopy," *WJGE*, vol. 5, no. 11, p. 534, 2013.

[45] M. Seong and S.-L. Chen, "Recent advances toward clinical applications of photoacoustic microscopy: a review," *Sci. China Life Sci.*, vol. 63, no. 12, pp. 1798–1812, Dec. 2020.

[46] A. A. Oraevsky, "Image reconstruction from photoacoustic projections," *Photonics Insights*, vol. 3, no. 4, p. C06, 2024.

[47] Y. Xu and L. V. Wang, "Time Reversal and Its Application to Tomography with Diffracting Sources," *Phys. Rev. Lett.*, vol. 92, no. 3, p. 033902, Jan. 2004.

[48] P. Burgholzer *et al.*, "Exact and approximative imaging methods for photoacoustic tomography using an arbitrary detection surface," *Phys. Rev. E*, vol. 75, no. 4, p. 046706, Apr. 2007.

[49] C. G. A. Hoelen *et al.*, "Three-dimensional photoacoustic imaging of blood vessels in tissue," *Opt. Lett.*, vol. 23, no. 8, p. 648, Apr. 1998.

[50] C. G. Hoelen *et al.*, "Photoacoustic blood cell detection and imaging of blood vessels in phantom tissue," presented at the BiOS Europe '97, H.-J. Foth, R. Marchesini, H. Podbielska, and A. Katzir, Eds., San Remo, Italy, Jan. 1998, pp. 142–153.

[51] R. A. Kruger *et al.*, "Photoacoustic ultrasound (PAUS)—Reconstruction tomography," *Medical Physics*, vol. 22, no. 10, pp. 1605–1609, Oct. 1995.

[52] Y. Guo *et al.*, "Deep learning for visual understanding: A review," *Neurocomputing*, vol. 187, pp. 27–48, Apr. 2016.

[53] M. Xu and L. V. Wang, "Universal back-projection algorithm for photoacoustic computed tomography," *Phys. Rev. E*, vol. 71, no. 1, p. 016706, Jan. 2005.

[54] C.-H. Tai *et al.*, "SE: an algorithm for deriving sequence alignment from a pair of superimposed structures," *BMC Bioinformatics*, vol. 10, no. S1, p. S4, Jan. 2009.

[55] R. Wang *et al.*, "Photoacoustic imaging with limited sampling: a review of machine learning approaches," *Biomed. Opt. Express*, vol. 14, no. 4, p. 1777, Apr. 2023.

[56] H. Shan *et al.*, "Simultaneous reconstruction of the initial pressure and sound speed in photoacoustic tomography using a deep-learning approach," in *Novel Optical Systems, Methods, and Applications XXII*, C. F. Hahlweg and J. R. Mulley, Eds., San Diego, United States: SPIE, Sep. 2019, p. 4.

[57] S. Ravishankar *et al.*, "Image Reconstruction: From Sparsity to Data-Adaptive Methods and Machine Learning," *Proc. IEEE*, vol. 108, no. 1, pp. 86–109, Jan. 2020.

[58] N. Davoudi *et al.*, "Deep learning optoacoustic tomography with sparse data," *Nat Mach Intell*, vol. 1, no. 10, pp. 453–460, Sep. 2019.

[59] M. Haltmeier *et al.*, "Photoacoustic image reconstruction via deep learning," in *Photons Plus Ultrasound: Imaging and Sensing 2018*, A. A. Oraevsky and L. V. Wang, Eds., San Francisco, United States: SPIE, Feb. 2018, p. 168.

[60] X. Wei *et al.*, "Deep learning-powered biomedical photoacoustic imaging," *Neurocomputing*, vol. 573, p. 127207, Mar. 2024.

[61] C. Yang *et al.*, "Review of deep learning for photoacoustic imaging," *Photoacoustics*, vol. 21, p. 100215, Mar. 2021.

[62] Q. Huang *et al.*, "A review of deep learning segmentation methods for carotid artery ultrasound images," *Neurocomputing*, vol. 545, p. 126298, Aug. 2023.

[63] J. Schmidhuber, "Deep learning in neural networks: An overview," *Neural Networks*, vol. 61, pp. 85–117, Jan. 2015.

[64] O. Ronneberger *et al.*, "U-Net: Convolutional Networks for Biomedical Image Segmentation," in *Medical Image Computing and Computer-Assisted Intervention – MICCAI 2015*, vol. 9351, N. Navab, J. Hornegger, W. M. Wells, and A. F. Frangi, Eds., in *Lecture Notes in Computer Science*, vol. 9351, Cham: Springer International Publishing, 2015, pp. 234–241.

[65] D. Allman *et al.*, "Photoacoustic Source Detection and Reflection Artifact Removal Enabled by Deep Learning," *IEEE Trans. Med. Imaging*, vol. 37, no. 6, pp. 1464–1477, Jun. 2018.

[66] S. Gutta *et al.*, "Deep neural network-based bandwidth enhancement of photoacoustic data," *J. Biomed. Opt.*, vol. 22, no. 11, p. 1.

[67] N. Awasthi *et al.*, "Deep Neural Network-Based Sinogram Super-Resolution and Bandwidth Enhancement for Limited-Data Photoacoustic Tomography," *IEEE Trans. Ultrason., Ferroelect., Freq. Contr.*, vol. 67, no. 12, pp. 2660–2673, Dec. 2020.

[68] D. A. Durairaj *et al.*, "Unsupervised deep learning approach for photoacoustic spectral unmixing," in *Photons Plus Ultrasound: Imaging and Sensing 2020*, A. A. Oraevsky and L. V. Wang, Eds., San Francisco, United States: SPIE, Feb. 2020, p. 125.

[69] J. Feng *et al.*, "End-to-end Res-Unet based reconstruction algorithm for photoacoustic imaging," *Biomed. Opt. Express*, vol. 11, no. 9, p. 5321, Sep. 2020.

[70] S. Guan *et al.*, "Fully Dense UNet for 2-D Sparse Photoacoustic Tomography Artifact Removal," *IEEE J. Biomed. Health Inform.*, vol. 24, no. 2, pp. 568–576, Feb. 2020.

[71] J. Zhang *et al.*, "Limited-View Photoacoustic Imaging Reconstruction With Dual Domain Inputs Based On Mutual Inforamtion," in *2021 IEEE 18th International Symposium on Biomedical Imaging (ISBI)*, Nice, France: IEEE, Apr. 2021, pp. 1522–1526.

[72] Lan H *et al.*, "A jointed feature fusion framework for photoacoustic image reconstruction," *Photoacoustics*, Feb; 29:100442, 2023.

[73] D. Zhang and A. Khoreva, "Progressive Augmentation of GANs," *arXiv*: 1901.10422, 2019.

[74] W. Zhong *et al.*, “Unsupervised disentanglement strategy for mitigating artifact in photoacoustic tomography under extremely sparse view,” *Photoacoustics*, vol. 38, p. 100613, Aug. 2024.

[75] X. Song *et al.*, “Accelerated model-based iterative reconstruction strategy for sparse-view photoacoustic tomography aided by multi-channel autoencoder priors,” *Journal of Biophotonics*, vol. 17, no. 1, p. e202300281, Jan. 2024.

[76] M. Guo *et al.*, “AS-Net: Fast Photoacoustic Reconstruction With Multi-Feature Fusion From Sparse Data,” *IEEE Trans. Comput. Imaging*, vol. 8, pp. 215–223, 2022.

[77] S. C. K. Chan *et al.*, “Local Spatial Attention Transformer For Sparse Photoacoustic Image Reconstruction,” in *2024 IEEE International Symposium on Biomedical Imaging (ISBI)*, Athens, Greece: IEEE, May 2024, pp. 1–5.

[78] T. Tong *et al.*, “Domain Transform Network for Photoacoustic Tomography from Limited-view and Sparsely Sampled Data,” *Photoacoustics*, vol. 19, p. 100190, Sep. 2020.

[79] H. Lan *et al.*, “Y-Net: Hybrid deep learning image reconstruction for photoacoustic tomography *in vivo*,” *Photoacoustics*, vol. 20, p. 100197, Dec. 2020.

[80] T. Vu *et al.*, “Deep image prior for undersampling high-speed photoacoustic microscopy,” 2020.

[81] D. Seong *et al.*, “Three-dimensional reconstructing undersampled photoacoustic microscopy images using deep learning,” *Photoacoustics*, vol. 29, p. 100429, Feb. 2023.

[82] B. Li *et al.*, “Removing Artifacts in Transcranial Photoacoustic Imaging With Polarized Self-Attention Dense-UNet,” *Ultrasound in Medicine & Biology*, vol. 50, no. 10, pp. 1530–1543, Oct. 2024.

[83] J. Wang *et al.*, “Reconstructing Cancellous Bone From Down-Sampled Optical-Resolution Photoacoustic Microscopy Images With Deep Learning,” *Ultrasound in Medicine & Biology*, vol. 50, no. 9, pp. 1459–1471, Sep. 2024.

[84] H. Shahid *et al.*, “Batch ReNormalization Accumulated Residual U-Network for Artifacts Removal in Photoacoustic Imaging,” in *2021 IEEE International Ultrasonics Symposium (IUS)*, Xi'an, China: IEEE, Sep. 2021, pp. 1–4.

[85] Y. Cao *et al.*, “Mean-reverting diffusion model-enhanced acoustic-resolution photoacoustic microscopy for resolution enhancement: Toward optical resolution,” *J. Innov. Opt. Health Sci.*, p. 2450023, Sep. 2024.

[86] T. D. Le *et al.*, “Enhanced resolution and sensitivity acoustic-resolution photoacoustic microscopy with semi/unsupervised GANs,” *Sci Rep*, vol. 13, no. 1, p. 13423, Aug. 2023.

[87] S. Cheng *et al.*, “High-resolution photoacoustic microscopy with deep penetration through learning,” *Photoacoustics*, vol. 25, p. 100314, Mar. 2022.

[88] H. Zhao *et al.*, “Deep Learning Enables Superior Photoacoustic Imaging at Ultralow Laser Dosages,” *Advanced Science*, vol. 8, no. 3, p. 2003097, Feb. 2021.

[89] M. Zhou *et al.*, “A Noise Reduction Method for Photoacoustic Imaging In Vivo Based on EMD and Conditional Mutual Information,” *IEEE Photonics J.*, vol. 11, no. 1, pp. 1–10, Feb. 2019.

[90] Y. Liu *et al.*, “UPAMNet: A unified network with deep knowledge priors for photoacoustic microscopy,” *Photoacoustics*, vol. 38, p. 100608, Aug. 2024.

[91] D. He *et al.*, “De-Noising of Photoacoustic Microscopy Images by Attentive Generative Adversarial Network,” *IEEE Trans. Med. Imaging*, vol. 42, no. 5, pp. 1349–1362, May 2023.

[92] J. Zhang *et al.*, “Organ-PAM: Photoacoustic Microscopy of Whole-organ Multiset Vessel Systems,” *Laser & Photonics Reviews*, vol. 17, no. 7, p. 2201031, Jul. 2023.

[93] Z. Zhang *et al.*, “Adaptive enhancement of acoustic resolution photoacoustic microscopy imaging via deep CNN prior,” *Photoacoustics*, vol. 30, p. 100484, Apr. 2023.

[94] J. Meng *et al.*, “Depth-extended acoustic-resolution photoacoustic microscopy based on a two-stage deep learning network,” *Biomed. Opt. Express*, vol. 13, no. 8, p. 4386, Aug. 2022.

[95] I. Loc and M. B. Unlu, “Speeding up Photoacoustic Imaging using Diffusion Models,” *arXiv*: 2312.08834, Oct. 17, 2024.

[96] W. Li *et al.*, “EndoSRR: a comprehensive multi-stage approach for endoscopic specular reflection removal,” *Int J CARS*, vol. 19, no. 6, pp. 1203–1211, Apr. 2024.

[97] M. Yeung *et al.*, “Focus U-Net: A novel dual attention-gated CNN for polyp segmentation during colonoscopy,” *Computers in Biology and Medicine*, vol. 137, p. 104815, Oct. 2021.

[98] G. Zhang *et al.*, “A Medical Endoscope Image Enhancement Method Based on Improved Weighted Guided Filtering,” *Mathematics*, vol. 10, no. 9, p. 1423, Apr. 2022.

[99] S. Moghtaderi *et al.*, “Endoscopic Image Enhancement: Wavelet Transform and Guided Filter Decomposition-Based Fusion Approach,” *J. Imaging*, vol. 10, no. 1, p. 28, Jan. 2024.

[100] Y. Wang *et al.*, “Photoacoustic/Ultrasound Endoscopic Imaging Reconstruction Algorithm Based on the Approximate Gaussian Acoustic Field,” *Biosensors*, vol. 12, no. 7, p. 463, Jun. 2022.

[101] J. Xiao *et al.*, “Acoustic-resolution-based spectroscopic photoacoustic endoscopy towards molecular imaging in deep tissues,” *Opt. Express*, vol. 30, no. 19, p. 35014, Sep. 2022.

[102] C. Yang *et al.*, “Quantitative Photoacoustic Blood Oxygenation Imaging Using Deep Residual And Recurrent Neural Network,” in *2019 IEEE 16th International Symposium on Biomedical Imaging (ISBI 2019)*, Venice, Italy: IEEE, Apr. 2019, pp. 741–744.

[103] R. Zhang *et al.*, “Navigating challenges and solutions in quantitative photoacoustic imaging,” *Applied Physics Reviews*, vol. 11, no. 3, p. 031308, Sep. 2024.

[104] M. Dantuma *et al.*, “Tunable blood oxygenation in the vascular anatomy of a semi-anthropomorphic photoacoustic breast phantom,” *J. Biomed. Opt.*, vol. 26, no. 03, Mar. 2021.

[105] X. Zhou *et al.*, “Evaluation of Fluence Correction Algorithms in Multispectral Photoacoustic Imaging,” *Photoacoustics*, vol. 19, p. 100181, Sep. 2020.

[106] L. Zhao *et al.*, “Optical fluence compensation for handheld photoacoustic probe: An *in vivo* human study case,” *J. Innov. Opt. Health Sci.*, vol. 10, no. 04, p. 1740002, Jul. 2017.

[107] M. Kirillin *et al.*, “Fluence compensation in raster-scan optoacoustic angiography,” *Photoacoustics*, vol. 8, pp. 59–67, Dec. 2017.

[108] T. Hirasawa *et al.*, “Multispectral photoacoustic imaging of tumours in mice injected with an enzyme-activatable photoacoustic probe,” *J. Opt.*, vol. 19, no. 1, p. 014002, Jan. 2017.

[109] J. C. Ranasinghesagara *et al.*, “Reflection-mode multiple-illumination photoacoustic sensing to estimate optical properties,” *Photoacoustics*, vol. 2, no. 1, pp. 33–38, Mar. 2014.

[110] H. Jin, R. Zhang *et al.*, “A Single Sensor Dual-Modality Photoacoustic Fusion Imaging for Compensation of Light Fluence Variation,” *IEEE Trans. Biomed. Eng.*, vol. 66, no. 6, pp. 1810–1813, Jun. 2019.

[111] T. Han, M. Yang *et al.*, “A three-dimensional modeling method for quantitative photoacoustic breast imaging with handheld probe,” *Photoacoustics*, vol. 21, p. 100222, Mar. 2021.

[112] A. M. Caravaca-Aguirre *et al.*, “High contrast three-dimensional photoacoustic imaging through scattering media by localized optical fluence enhancement,” *Opt. Express*, vol. 21, no. 22, p. 26671, Nov. 2013.

[113] M. N. Fadhel *et al.*, “Fluence-matching technique using photoacoustic radiofrequency spectra for improving estimates of oxygen saturation,” *Photoacoustics*, vol. 19, p. 100182, Sep. 2020.

[114] A. Dolet *et al.*, “In Vitro and In Vivo Multispectral Photoacoustic Imaging for the Evaluation of Chromophore Concentration,” *Sensors*, vol. 21, no. 10, p. 3366, May 2021.

[115] M. U. Arabul *et al.*, “Unmixing multi-spectral photoacoustic sources in human carotid plaques using non-negative independent component analysis,” *Photoacoustics*, vol. 15, p. 100140, Sep. 2019.

[116] C. Shi and L. Wang, “Incorporating spatial information in spectral unmixing: A review,” *Remote Sensing of Environment*, vol. 149, pp. 70–87, Jun. 2014.

[117] S. Tzoumas and V. Ntziachristos, “Spectral unmixing techniques for optoacoustic imaging of tissue pathophysiology,” *Phil. Trans. R. Soc. A*, vol. 375, no. 2107, p. 20170262, Nov. 2017.

[118] T. Feng *et al.*, “Detection of collagen by multi-wavelength photoacoustic analysis as a biomarker for bone health assessment,” *Photoacoustics*, vol. 24, p. 100296, Dec. 2021.

[119] S. Tzoumas *et al.*, “Eigenspectra optoacoustic tomography achieves quantitative blood oxygenation imaging deep in tissues,” *Nat Commun*, vol. 7, no. 1, p. 12121, Jun. 2016.

[120] M. S. Karoui *et al.*, “Blind spatial unmixing of multispectral images: New methods combining sparse component analysis, clustering and non-negativity constraints,” *Pattern Recognition*, vol. 45, no. 12, pp. 4263–4278, Dec. 2012.

[121] T. Kirchner *et al.*, “Context encoding enables machine learning-based quantitative photoacoustics,” *J. Biomed. Opt.*, vol. 23, no. 05, p. 1, May 2018.

[122] C. Cai *et al.*, "End-to-end deep neural network for optical inversion in quantitative photoacoustic imaging," *Opt. Lett.*, vol. 43, no. 12, p. 2752, Jun. 2018.

[123] I. Olefir *et al.*, "Deep Learning-Based Spectral Unmixing for Optoacoustic Imaging of Tissue Oxygen Saturation," *IEEE Trans. Med. Imaging*, vol. 39, no. 11, pp. 3643–3654, Nov. 2020.

[124] N. T. Huynh *et al.*, "A fast all-optical 3D photoacoustic scanner for clinical vascular imaging," *Nat. Biomed. Eng.*, Sep. 2024.

[125] Dong, Chao *et al.* "Image Super-Resolution Using Deep Convolutional Networks." *IEEE Transactions on Pattern Analysis and Machine Intelligence* 38 (2014): 295-307.

[126] C. Dong *et al.*, "Learning a Deep Convolutional Network for Image Super-Resolution," in *Computer Vision – ECCV 2014*, vol. 8692, D. Fleet, T. Pajdla, B. Schiele, and T. Tuytelaars, Eds., in Lecture Notes in Computer Science, vol. 8692., Cham: Springer International Publishing, 2014, pp. 184–199.

[127] C. Ledig *et al.*, "Photo-Realistic Single Image Super-Resolution Using a Generative Adversarial Network," in *2017 IEEE Conference on Computer Vision and Pattern Recognition (CVPR)*, Honolulu, HI: IEEE, Jul. 2017, pp. 105–114.

[128] Y. Wang *et al.*, "CAMixerSR: Only Details Need More ‘Attention’," 2024 IEEE/CVF Conference on Computer Vision and Pattern Recognition (CVPR), Seattle, WA, USA, 2024, pp. 25837-25846.

[129] H. Sun *et al.*, "CoSeR: Bridging Image and Language for Cognitive Super-Resolution," 2024 IEEE/CVF Conference on Computer Vision and Pattern Recognition (CVPR), Seattle, WA, USA, 2024, pp. 25868-25878.

[130] J. Kim *et al.*, "Accurate Image Super-Resolution Using Very Deep Convolutional Networks," in *2016 IEEE Conference on Computer Vision and Pattern Recognition (CVPR)*, Las Vegas, NV, USA: IEEE, Jun. 2016, pp. 1646–1654.

[131] Y. Tai *et al.*, "Image Super-Resolution via Deep Recursive Residual Network," in *2017 IEEE Conference on Computer Vision and Pattern Recognition (CVPR)*, Honolulu, HI: IEEE, Jul. 2017, pp. 2790–2798.

[132] Liu *et al.*, "Residual Feature Distillation Network for Lightweight Image Super-Resolution." arXiv arXiv, 2020.

[133] C. Wang *et al.*, "Transform Domain Based Medical Image Super-resolution via Deep Multi-scale Network," in *ICASSP 2019 - 2019 IEEE International Conference on Acoustics, Speech and Signal Processing (ICASSP)*, Brighton, United Kingdom: IEEE, May 2019, pp. 2387–2391.

[134] K. Shen *et al.*, "Physics-driven deep learning photoacoustic tomography," *Fundamental Research*, p. S2667325824003583, Sep. 2024.

[135] F. Zhu and W. Liu, "A novel medical image fusion method based on multi-scale shearing rolling weighted guided image filter," *MBE*, vol. 20, no. 8, pp. 15374–15406, 2023.

[136] J. Ma *et al.*, "GANMcC: A Generative Adversarial Network With Multiclassification Constraints for Infrared and Visible Image Fusion," *IEEE Trans. Instrum. Meas.*, vol. 70, pp. 1–14, 2021.

[137] N. Nyayapathi *et al.*, "Dual-modal photoacoustic and ultrasound imaging: from preclinical to clinical applications," *Front. Photon.*, vol. 5, p. 1359784, Feb. 2024.

[138] Y. Notsuka *et al.*, "Improvement of spatial resolution in photoacoustic microscopy using transmissive adaptive optics with a low-frequency ultrasound transducer," *Opt. Express*, vol. 30, no. 2, p. 2933, Jan. 2022.

[139] S. K. Biswas *et al.*, "A Method for Delineation of Bone Surfaces in Photoacoustic Computed Tomography of the Finger," *Ultrason. Imaging*, vol. 38, no. 1, pp. 63–76, Jan. 2016.

[140] T. D. Le, S.-Y. Kwon, and C. Lee, "Segmentation and Quantitative Analysis of Photoacoustic Imaging: A Review," *Photonics*, vol. 9, no. 3, p. 176, Mar. 2022.